Soft Matter

PAPER

View Article Online
View Journal | View Issue

Cite this: *Soft Matter*, 2019, **15**, 3379

# Designing bijels formed by solvent transfer induced phase separation with functional nanoparticles†

Stephen Boakye-Ansah,* Matthew S. Schwenger and Martin F. Haase

Received 10th February 2019,
Accepted 24th March 2019

DOI: 10.1039/c9sm00289h

rsc.li/soft-matter-journal

Bicontinuous interfacially jammed emulsion gels (bijels) formed *via* solvent transfer induced phase separation (STrIPS) are new soft materials with potential applications in separations, healthcare, or catalysis. To facilitate their applications, means to fabricate STrIPS bijels with nanoparticles of various surface chemistries are needed. Here, we investigate the formation of STrIPS bijels with nanoparticles of different wettabilities, ranging from partially hydrophobic to extremely hydrophilic. To this end, the surface wettability of silica nanoparticles is tailored by functionalization with ligands bearing either hydrophobic or hydrophilic terminal groups. We show that partially hydrophobic particles with acrylate groups can impart short-term stability to STrIPS bijels on their own. However, to enable long-term stability, the use of cationic surfactants is needed. Partially hydrophobic particles require short chain surfactants for morphological stability while glycerol-functionalized hydrophilic particles require double chain cationic surfactants. Variation of the surfactant concentration results in various STrIPS bijel morphologies with controllable domain sizes. Last, we show that functional groups on the nanoparticles facilitate interfacial cross-linking for the purposes of reinforcing STrIPS bijels. Our research lays the foundation for the use of a wide variety of solid particles, irrespective of their surface wettabilities, to fabricate bijels with potential applications in Pickering interfacial catalysis and as cross-flow microreactors.

## 1 Introduction

The discovery of bicontinuous interfacially jammed emulsion gels (bijels) provided a pathway for the synthesis of static interpenetrating biphasic liquid microstructures.[1–3] These structures are stabilized at the interface by a percolating layer of colloidal particles. Bijel-derived materials present interesting features such as high surface area, high porosity, structural tunability, high particle loadings, and easy fabrication, which make them highly attractive for applications including sensor technologies,[4] separation processes,[5] tissue engineering,[6] battery electrodes,[7] and fuel cells.[8] By transforming bijels into polymeric materials, researchers have derived useful materials such as hierarchical porous templates,[9] electrode materials for both supercapacitor and fuel cells,[8,10,11] porous hydrogels for biomedical applications[6] and multifunctional nanocomposite membranes for water purification.[5]

The formation of bijels typically involves the interfacial arrest of two immiscible liquids undergoing spinodal decomposition which are mechanically stabilized in a non-equilibrium configuration by a jammed monolayer of colloidal particles at their interface.[1,2] As first experimentally demonstrated by Herzig *et al.*, thermal quenching of binary liquid mixtures resulted in the formation of bijels characterized by large domain sizes ($\sim 40\ \mu$m).[2] By using smaller-sized particles ($<100$ nm), bijels with sub-micrometre domains have also been realized, contributing to the generation of bicontinuous morphologies with high surface areas.[12–15]

Moreover, Composto and coworkers have also demonstrated the control of polymeric bicontinuous morphologies *via* the segregation and jamming of nanoparticles at the interphase of polymer blends undergoing phase separation.[16,17] For example, the partitioning behaviour of polymer-grafted silica nanoparticles (SNPs) depended on both the chain length and the end group of the polymer-brush, which also determined the morphology of the nanocomposite material.[17]

Solid particles used for bijel stabilization typically have spherical shapes,[2,12,15,18] but rod-shaped particles,[19] 2D graphene oxide sheets,[20] and microbial cells[21] can also stabilize bijels. Incorporating nanoparticles into bicontinuous materials not only imparts functional properties, but also the type, shape, and surface properties of the particles can be used to control their morphology. An example is what Hayward *et al.* showed,

---

*Rowan University, Henry M. Rowan College of Engineering, Department of Chemical Engineering, 201 Mullica Hill Rd, Glassboro, NJ 08028, USA. E-mail: haasem@rowan.edu*

† Electronic supplementary information (ESI) available. See DOI: 10.1039/c9sm00289h

that beside interfacial jamming of particles, colloidal gelation in one phase of a polymer blend could arrest bicontinuous structures.[22] The shape of the particles (nanorods or nanospheres) affected the morphology,[22] similar to what Clegg *et al.* observed for bijels formed by phase separation.[19]

Recently, new approaches to simplify the fabrication of bijels by circumventing the limitations of thermal quenching have been introduced. Haase *et al.* introduced Solvent Transfer Induced Phase Separation (STrIPS) for the fabrication of hierarchical and asymmetric bijel fibers, particles and films.[5,14,23] STrIPS generates bijels out of a broad selection of immiscible liquid combinations, since a solvent is used to create the initial homogeneous mixture of the immiscible liquids undergoing phase separation.

The next dramatic step in simplifying bijel formation was taken independently from each other by Cai *et al.*, as well as Huang *et al.* They discovered that bijels can be formed by simply shaking up a mixture of two immiscible fluids with surface-active particles. These advances further broaden the selection of immiscible liquids deployable to form bijels. Cai *et al.* introduced a multistep homogenization procedure with fluids of increased viscosities.[15] The different approach by Huang *et al.* employs nanoparticle surfactants with polymeric surface modifiers of different molecular weights.[13]

The new approaches of forming bijels either by STrIPS or simple shaking have a key step to simplify bijel formation in common: The use of surfactants to adjust the wettability of the nanoparticles *in situ* for the liquid scaffold stabilization.[5,13–15] *In situ* surface modification allows for a simple control over the nanoparticle wettability, essential for bijel stabilization, as the particles are required to adopt a near-neutral contact angle (CA $\sim$ 90°) to stabilize the percolating interface.[1,24]

Though extensive work has been done on the stabilization of discrete emulsion droplets with either hydrophilic or hydrophobic particles *via* the *in situ* surfactant modification of nanoparticles,[25–31] research on the requirements to stabilize bijels with particles of different initial wettability by action of *in situ* modifiers is limited. Research on the bijel structure dependence on the initial particle wetting properties is of great interest for many applications since, for example, catalyst particles intended for use in bijel based Pickering interfacial catalysis can have a wide range of surface wettabilities.[32,33]

Here, we investigate the criteria for the *in situ* surface modification of nanoparticles of different initial wettabilities to stabilize bijels formed by Solvent Transfer Induced Phase Separation (STrIPS). For our study we tune the initial wettability of model silica particles from (i) moderately hydrophobic to (ii) strongly hydrophilic. Then, we investigate the type and concentration of *in situ* modifying quaternary ammonium surfactants allowing for bijel formation with these particles. Silica particles are functionalized with hydrophobic 3-(trimethoxysilyl)-propyl acrylate groups, and hydrophilic 3-glycidoxypropyltrimethoxysilane groups (see schematic in Fig. 1a). This wide range of initial surface properties is proposed as a model system to mimic the stabilization of bijels with potential catalyst particles.[33–38]

Surprisingly, we find that acrylate functionalized silica nanoparticles allow for the temporary stabilization of STrIPS bijels without the use of *in situ* surface modifiers. However, to obtain long term stability, *in situ* surface modification of the nanoparticles with short chain quaternary ammonium surfactants is needed. Moreover, we show how extremely hydrophilic glycerol-coated nanoparticles require strongly hydrophobic quaternary ammonium surfactants as *in situ* modifiers to stabilize bijels.

Last, we demonstrate how bijels with functionalized nanoparticles enhance bijel stability over wide pH ranges by cross-linking the interfacial particles. By functionalizing the particles used for making bijels, novel, robust, and versatile bijel materials can be derived for diverse applications such as drug encapsulation, controlled release of active ingredients, and Pickering interfacial catalysis.

## 2 Experimental methods

### 2.1 Materials

Silica nanoparticles (22 nm Ludox TMA), hexadecyl-trimethylammonium bromide ($C_{16}$TAB) with purity >98%, dihexadecyl dimethylammonium bromide $(C_{16})_2$TAB, dodecyl trimethylammonium bromide ($C_{12}$TAB), diethyl phthalate (DEP, 99.5%), Nile Red, 2-hydroxy-2-methylpropiophenone (HMPP), 1,4 butanediol diacrylate (BDA), deionized water and pure ethanol 200 proof (>99.5%) were used for all experiments. 3-(Trimethoxysilyl)propyl acrylate (TPA, 92%) and 3 glycidoxypropyl-trimethoxy silane (GPO, ≥98%) were purchased from Sigma-Aldrich and used as received.

### 2.2 Surface modification of silica nanoparticles

Silica nanoparticle dispersions, comprising water (33.3 v/v), ethanol (38.1 v/v), acetic acid (33.3 v/v) and Ludox TMA (9.5 v/v) were mixed in tightly sealed glass bottles and placed in a 70 °C heating bath under constant stirring. Nitrogen was bubbled through the mixture for 10 min. To functionalize the nanoparticles, calculated concentrations of functional monomers (3-trimethoxy propyl acrylate (TPA) or 3-glycidoxypropyltrimethoxysilane (GPO)) were introduced to the nanoparticle dispersions and stirred over-night, resulting in the silanization of hydrophobic (acrylate) or hydrophilic (glycerol) nanoparticles. After 12 hours, DI water of same volume as the reactant mixture was added to the acrylate-functionalized silica nanoparticles, resulting in particle sedimentation. The sediment was subsequently washed in DI water for three consecutive times (centrifugation, redispersion cycles). After the last washing step, the aqueous supernatant was decanted, and ethanol was added to the sediment. The samples were shaken vigorously and ultra-sonicated to re-disperse the functionalized particles, followed by dialysis in ethanol (200 proof) for 12 hours. For glycerol-functionalized particles, the reaction mixture was partially evaporated to half of its original volume after 12 hours reaction. Then, washing was realized by three sequential dialysis steps in water at pH 3.

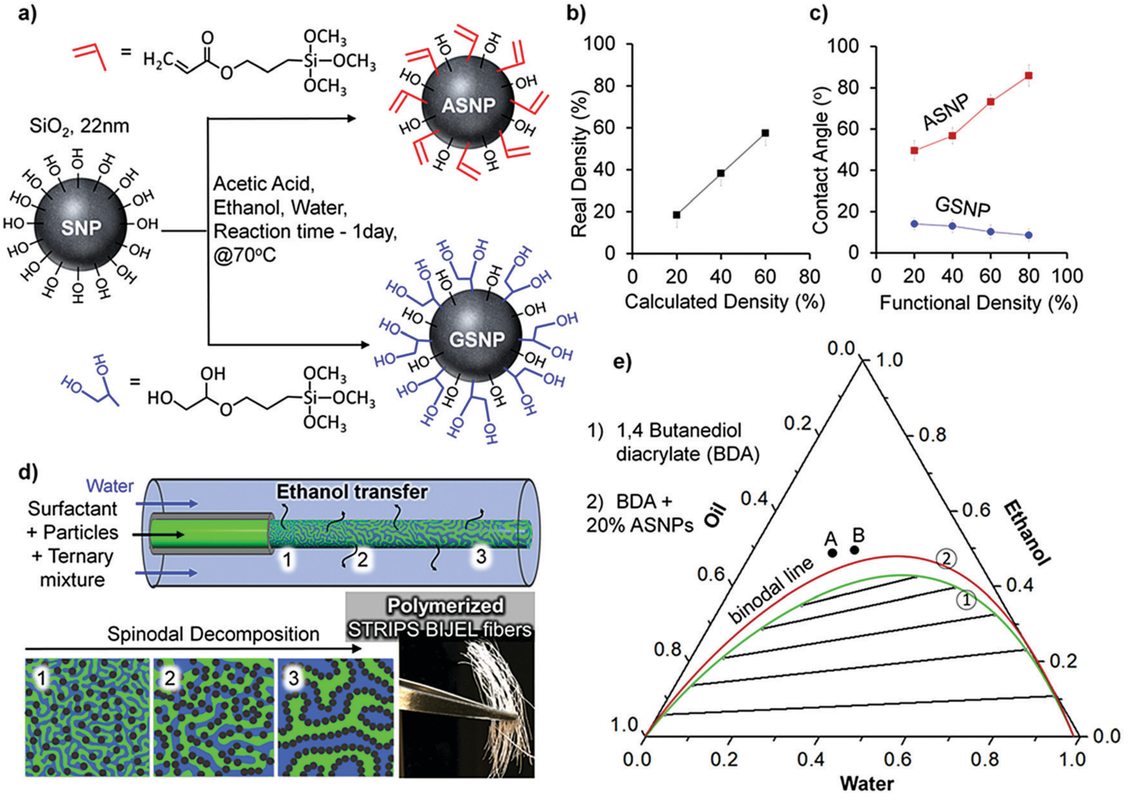

Fig. 1 Nanoparticle modification and STRIPS bijel fabrication. (a) Surface modification of 22 nm Ludox TMA silica nanoparticles (SNP) with acrylate or glycerol groups, rendering the particles partially hydrophobic (ASNP) or hydrophilic (GSNP) respectively. (b) Results from acid–base titration experiments to derive the percentage of silanol groups on functionalized SNPs. (c) Results from sessile drop contact angle measurements for both acrylate and glycerol functionalized particles of varying degree of functionalization (conducted on a thin film deposition of functionalized particle dispersion on a glass slide). (d) Fabrication method of STRIPS bijels by co-axial extrusion of ternary mixtures into a stream of water within a coaxial microcapillary device. (e) Measured ternary phase diagram with binodal and tie lines of the liquid system, oil (1,4 butanediol diacrylate (BDA)), water and solvent (ethanol). The initial ternary compositions used for STrIPS in this work is indicated by the black points on the binodal line ("A" for 20% – ASNP and "B" for both 40% and 60% – ASNPs). The binodal line position of BDA (indicated as (1)), is moved upwards due to the addition of hydrophobic acrylate functionalized silica nanoparticles (indicated as (2)).

### 2.3 Preparation of stock solutions

Dialyzed concentrates of acrylated particles in ethanol and glycerol particles in water (both ∼50 wt% particles) are used as stock dispersions. To prepare surfactant solutions, calculated molar concentrations of the chosen surfactants (∼100 mM $(C_{16})_2TAB$, ∼200 mM for $C_{16}TAB$ and $C_{12}TAB$) are prepared in ethanol (200 proof).

### 2.4 Ternary liquid mixture preparation and bijel fabrication

1.5 ml of ternary fluid mixtures at critical compositions of the oil, water, and solvent are prepared and mixed together with the functionalized silica nanoparticles (wt% = 37.5), which are used to fabricate the STrIPS bijels. The fractions of oil ($\varphi_o$), water ($\varphi_w$) and ethanol ($\varphi_e$) used to prepare the ternary mixtures for each of the acrylate particles were as follows: 20%-ASNPs ($\varphi_o$ = 0.32, $\varphi_w$ = 0.18, and $\varphi_e$ = 0.50) and for 40%- and 60%-ASNPs ($\varphi_o$ = 0.27, $\varphi_w$ = 0.24 and $\varphi_e$ = 0.49), indicated as points "A" and "B" respectively in Fig. 1e. For the ternary mixtures made with the hydrophobic acrylated silica nanoparticles (20%, 40% and 60%), STrIPS bijel fibers were fabricated with or without the inclusion of surfactants. When surfactants were required, molar concentrations of the cationic alkyl surfactants (cetyltrimethyl-ammonium bromide) were used accordingly. For hydrophilic glycerol-functionalized silica nanoparticles (GSNPs), we varied both the surfactant type (hydrocarbon chain and length) and their respective concentrations when the ternary mixtures were prepared. The bijel fiber extrusion process entailed the use of custom made microcapillary devices with polymeric coatings, as earlier reported.[14] To polymerize the fabricated STrIPS bijel fibers, we added the photo initiator (HMPP) to the ternary mixture compositions and exposed them to UV light (∼5 minutes), resulting in the conversion of the monomeric oil phase (BDA) into a solid polymer.

### 2.5 Characterization

To obtain high resolution confocal laser scanning micrographs (CLSM) of the polymerized bijel fibers, we conducted refractive index (RI) matching by soaking the UV-polymerized fibers in ethanol (200 proof) overnight and subsequently in diethyl phthalate (DEP). Highly pixelated confocal images were obtained after the confocal scans, 3D reconstructions of the bijel structures are made to obtain efficient characterization of the bicontinuous morphologies. We crop the z-stack high resolution images of the resulting CLSM data in a stepwise fashion and process them into three-dimensional figures. Sessile drop contact angle measurements are taken for each of the functionalized SNPs by using an optical tensiometer (Attention Theta, by Biolin Scientific), operated at room temperature. A thin film of either hydrophobic (ASNPs) or hydrophilic (GSNPs) particles dispersed in ethanol is spread on a glass slide and dried for approximately 30 minutes. Drops of DI water are deposited on the nanoparticle films and the resulting contact angles measured. For the glycerol functionalized nanoparticles (1 wt%), zeta potential measurements in dependence of pH are carried out to investigate their surface charges (of 20%-GSNPs and 90%-GSNPs) by using a Malvern Zetasizer 200 instrument at 25 °C. The pH is adjusted by adding 0.1 M NaOH to the aqueous particle dispersions under constant stirring. To characterize robust GSNP-bijels, CLSM was used to obtain time series of bijel structures (crosslinked and non-crosslinked) affected by increase in pH. A high-speed camera connected to an optical microscope (Nikon Diaphot 300) was used to capture micrographs of bijels undergoing fluid remixing.

# 3 Results and discussion

Controlled initial wettabilities of nanoparticles are obtained by treatment with organofunctional alkoxysilane molecules. To this end, 22 nm sized Ludox TMA silica nanoparticles (SNPs) are silanized with either 3-(trimethoxysilyl)propyl acrylate (TPA) or glycidoxypropyl trimethoxy silane (GPO) to render the particles partially hydrophobic (TPA) or hydrophilic (GPO) (see schematic in Fig. 1a). Specific concentrations of TPA or GPO are introduced in a reaction vessel containing water, ethanol, acetic acid, and a dispersed fraction of the Ludox nanoparticles. The amounts of TPA or GPO added are selected based on the calculated amounts of silanol groups on the nanoparticles (see Fig. SI1 and Supplementary Note 1, ESI†).[39] We define the percentage of coverage as the degree of TPA or GPO added to functionalize a corresponding stoichiometric percentage of silanol groups on the nanoparticles. Fig. 1b shows the results of our acid–base titrations, revealing that the added percentages of TPA translate to $\sim$ 94% coverage of the available silanol groups (see Supplementary Note 2, ESI†).

The stark contrast in wettability for the acrylate functionalized nanoparticles (ASNPs) and glycerol functionalized nanoparticles (GSNPs) is demonstrated by macroscopic contact angle measurements at a pH value of $\sim$3. A thin particle film is deposited on a glass slide and the contact angle of a sessile water droplet on the film is measured. Fig. 1c shows that the contact angles for ASNPs range from 50–90 degrees, indicating their partially hydrophobic character. Importantly, an increase of the degree of acrylate functionalization increases the contact angle and hydrophobic nature. In contrast, the contact angles for the GSNPs range from 5 to 15 degrees, indicating their hydrophilic character (Fig. 1c).

In our study, bijels are generated *via* Solvent Transfer Induced Phase Separation (STrIPS).[14] STrIPS requires the rapid injection of a homogeneous ternary mixture into a continuous stream of water to make bijels. The hydrophobic (oil) and hydrophilic (water) components are mixed *via* a solvent (ethanol), which includes a dispersed suspension of functionalized nanoparticles to make a homogeneous ternary mixture. When the ternary mixture is extruded into a continuous stream of water, the solvent (ethanol) is extracted into the surrounding water, leading to phase separation. As demixing proceeds, the nanoparticles are swept onto the liquid–liquid interface, where they accumulate and jam to arrest the bicontinuous oil/water network (see schematic in Fig. 1d). Continuously fabricated STrIPS bijel fibers can be polymerized and used for multiple applications.[5,14]

In the following, we present the results of our investigation of stabilizing STrIPS bijels, first with acrylate-functionalized particles, and second with glycerol functionalized particles. It is important to stress that our results are valid for particles with surfaces conditioned at acidic pH value ($\mathrm{pH} < 3$). Here, the majority of the remaining silanol groups of the partially functionalized silica nanoparticles are protonated.

### 3.1 Stabilization of bijels with partially hydrophobic (acrylate functionalized) nanoparticles

Acrylated nanoparticles are found to affect the ternary liquid phase equilibrium by decreasing the miscibility. A suspension of ASNPs in ethanol is mixed with 1,4 butanediol diacrylate (BDA), pure ethanol, and water. A miscible particle-ternary mixture suspension remains clear, indicating homogeneous particle dispersion and effective mixing of the liquid and solid components. The miscibility of the mixture is dictated by the binodal line (indicated as (2)) in the ternary liquid phase diagram displayed in Fig. 1e. In contrast to the liquid mixture composed of only the liquids BDA, ethanol, and water (indicated as (1)), the binodal line is shifted upwards with added acrylated particles. This is likely due to the overall increase in the hydrophobic constituents (oil (BDA) + acrylate particles) included in the ternary mixture, which required a corresponding increase in the fraction of ethanol needed for homogeneous mixing.

Solvent Transfer Induced Phase Separation (STrIPS) is carried out with ternary compositions indicated in the ternary phase diagram, as indicated by the points, ''A'' for 20%-ASNP and ''B'' for both 40% and 60%-ASNPs (see Fig. 1e), plus 0.4 wt% of the radical photo initiator 2-hydroxy-2-methylpropiophenone (HMPP) and $<$0.1 wt% Nile Red. The ternary mixtures are extruded as fibers *via* a coaxial glass capillary device and collected in a water-filled vial.[14] Within less than two minutes after extrusion, the fibers are irradiated with high intensity UV-light (5 min, 340 nm, $>$20 W cm$^{-2}$) for polymerization of the BDA. The polymerized fibers are washed with ethanol and immersed in diethyl phthalate to obtain optical transparency for further characterization.

Confocal laser scanning microscopy (CLSM) reveals well-defined bicontinuous channel morphologies for all degrees of

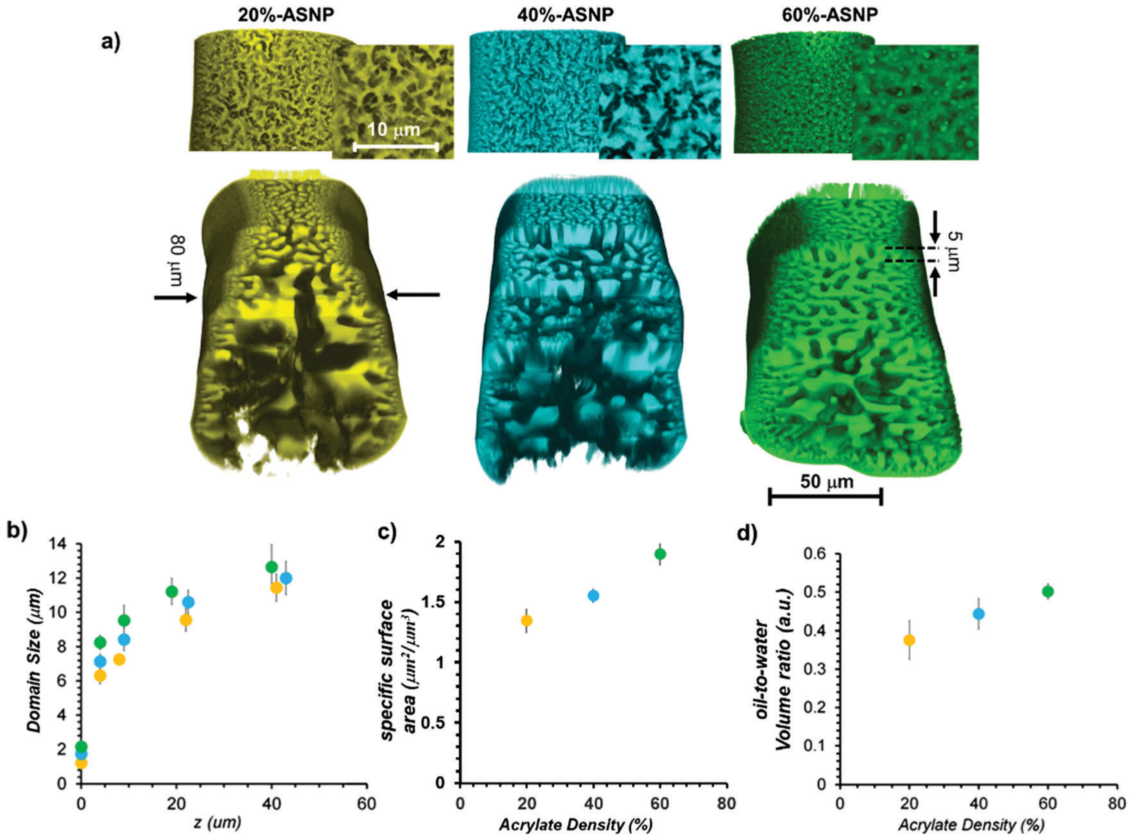

Fig. 2 STrIPS bijels stabilized solely with acrylate functionalized silica nanoparticles (ASNPs). (a) 3D confocal laser scanning microscopy reconstructions of surfactant-free STrIPS bijel fibers. The 3D reconstructions of the cylindrical fibers were cut at different height levels to reveal the internal morphologies (see Supplementary Methods, ESI†). Samples were fabricated by using particles with varying acrylate densities (20%-ASNP, 40%-ASNP and 60%-ASNP). (b) Oil domain size measurements with respect to confocal z positions of the respective ASNP-STrIPS bijel fibers in (a), where the data points are indicated by the respective colour codes of the fiber segments. (c) The surface area measurements are estimated using 2D image analysis of equatorial slices of the respective fiber segments (also, see Supplementary Note 3, ESI†). (d) The oil-to-water volume ratio of the fibers are estimated from 2D image analysis of the equatorial slices from each of the fiber segments in (a) (also see Supplementary Note 3, ESI†). The error bars correspond to standard deviations of five measurements.

acrylation investigated here (20%-ASNP, 40%-ASNP and 60%-ASNP) (Fig. 2). This finding shows how the inherent hydrophobicity of the ASNPs enables the stabilization of bicontinuous liquid structures by the particles alone. Our result contrasts with previous findings, where the addition of cationic surfactants in combination with unmodified silica particles was needed to obtain bijel morphologies.[5,14,32]

The fibers have asymmetric pore size distributions, with small pores at the surface and larger pores towards the inside. This trend is quantified in Fig. 2b, showing measurements of the oil domain sizes from the surface (at 0 µm) to the equatorial regions (at ∼40 µm). Similar asymmetric structures of STrIPS bijels have been found in earlier reports with surfactant-modified particles,[5,14] further extending their potential applications in separations, especially where size-selective transport is required.[40]

The internal oil domains become larger in size, show more interconnectivity, and more strongly resemble the spinodal patterns of the phase separation with increasing degree of particle acrylation (Fig. 2a). The presence of more spinodal patterns, for example in 60%-ASNP, is likely what contributes to the overall increase in STrIPS bijel surface area when the acrylate density is increased, which is quantified in Fig. 2c (see Supplementary Note 3, ESI†). Also, a possible explanation for the increased volume of the oil domains is that with more hydrophobic particles, enhanced particle partitioning into the oil-rich phase takes place. Correspondingly, the oil-to-water volume ratio increases with respect to an increase in the acrylate density, as quantified in Fig. 2d.

When left unpolymerized, bijels formed with acrylated particles alone coarsen over time (Fig. 3). This coarsening process is significantly slower (min to tens of min) than the spinodal phase separation (milliseconds to seconds), indicating a gradual rearrangement of the interfacial nanoparticles. Interestingly, the coarsening dynamics are slower with particles of increasing acrylation degree. 60%-ASNP STrIPS-bijels are most stable (for up to 15 minutes), followed by 40%-ASNP (6 minutes) and lastly, 20%-ASNP (only up to 2 minutes). Long-term stability of bijels formed with acrylated particles can be achieved *via* addition of cationic surfactants. The coarsening observed in Fig. 3 does not take place when 1 mM hexadecyltrimethylammonium bromide ($C_{16}TAB$) is added to the continuous

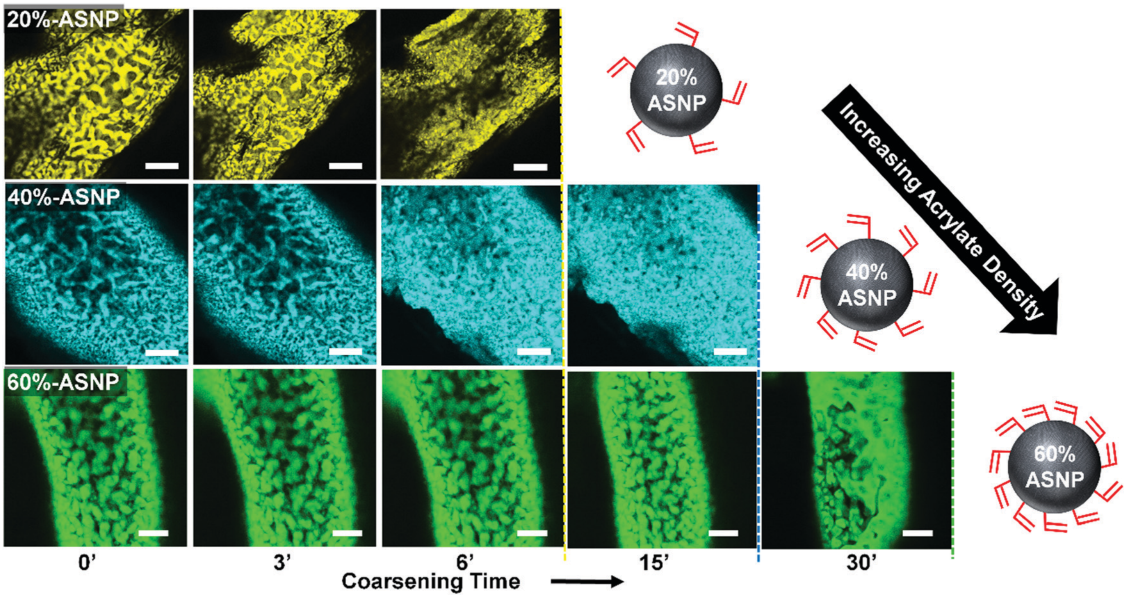

Fig. 3 Coarsening dynamics of STrIPS-bijels stabilized with acrylate silica nanoparticles. Confocal laser scanning microscopy time series of coarsening bijels stabilized solely with acrylate functionalized silica nanoparticles. Onset of bijel destabilization decreases with decreasing degree of acrylate functionalization (15 min for $\rho_{60\%}$, >6 min for $\rho_{40\%}$ and >3 min for $\rho_{20\%}$). Scale bar corresponds to 20 μm.

external water phase. It is likely that the remaining silanol (SiOH) groups on the surface of the nanoparticles serve as physisorption sites for the $C_{16}$TAB molecules, rendering them sufficiently interfacially active to permanently stabilize the bijel structure. On the other hand, irrespective of the degree of acrylation, the direct addition of $C_{16}$TAB to the ternary mixture does not allow for bijel formation, and instead results in viscoelastic oil structures with interspersed water droplets, rather than bicontinuous channels (see Supplementary Note 4, ESI†). This indicates excessive hydrophobicity imparted to the particles by $C_{16}$TAB adsorption from the ternary mixture, resulting in the formation of water-in-oil emulsions.

By replacing $C_{16}$TAB with dodecyltrimethylammonium bromide ($C_{12}$TAB), long term stability of STrIPS bijels with controllable bicontinuous morphology can be achieved. We study the effect of $C_{12}$TAB addition to the initial ternary mixture in the following. Fig. 4 shows confocal 3D reconstructions of STrIPS bijels fabricated with particles of variable degrees of acrylation in dependence of the $C_{12}$TAB concentrations in the initial ternary casting mixture. As opposed to $C_{16}$TAB, a wider range of surfactant concentrations facilitates the formation of nodular bicontinuous within the fibers. For example, for 20%-ASNPs, up to ~40 mM $C_{12}$TAB results in the formation of bicontinuous structures.

The initial hydrophobicity of the nanoparticles determines the maximum allowable additional hydrophobicity imparted by the surfactant for bijel stabilization. For each degree of particle acrylation, a characteristic threshold exists, above which no bicontinuous nodular oil/water channels can be formed. The higher the degree of acrylation, the lower this threshold surfactant concentration. Bijels are not formed for 60%-ASNPs above 20 mM $C_{12}$TAB, for 40% ASNPs above 30 mM $C_{12}$TAB or for 20% ASNPs above 45 mM $C_{12}$TAB. It is likely that above these threshold surfactant concentrations, excessive adsorption of $C_{12}$TAB renders the nanoparticles too hydrophobic to stabilize bicontinuous structures. This finding indicates that the initial hydrophobicity of the nanoparticles puts a limit to the additional hydrophobicity imparted by the surfactant.

The surface pore sizes of the ASNP bijel fibers decrease with an increase in the surfactant ($C_{12}$TAB) concentration in the range below the concentration threshold, whereas their surface oil domain sizes increase with an increase in the degree of acrylation and pH (see Supplementary Note 5, ESI†).

An interesting observation is that with added $C_{12}$TAB, the bijel fibers often have hollow interiors (Fig. 4). We believe, this can be related to the accumulation of water rich phase in the centre of the fiber during STrIPS. Electron microscopy shows that the surface pores of the bijels formed with $C_{12}$TAB are clogged by aggregated excess silica particles. This pore clogging can result in a significant barrier for the diffusion of solvent to the external water phase. As a result, the solvent is trapped in the middle of the fiber and generates a hollow interior.

This pore clogging effect can be suppressed in part by the addition of propanol to the continuous water phase. SEM images show that with the addition of 10 vol% propanol, open surface pore structures are formed (see Fig. SI8 in Supplementary Note 6, ESI†). This finding is analogous to the pore opening effect with ethanol addition to the continuous phase found in previous reports.[5] However, in the present work, ethanol addition did not open the surface pores as significantly as propanol. A possible explanation is that propanol reduces the aggregation of the acrylate functionalized particles by suppressing the interaction of the adsorbed $C_{12}$TAB chains.

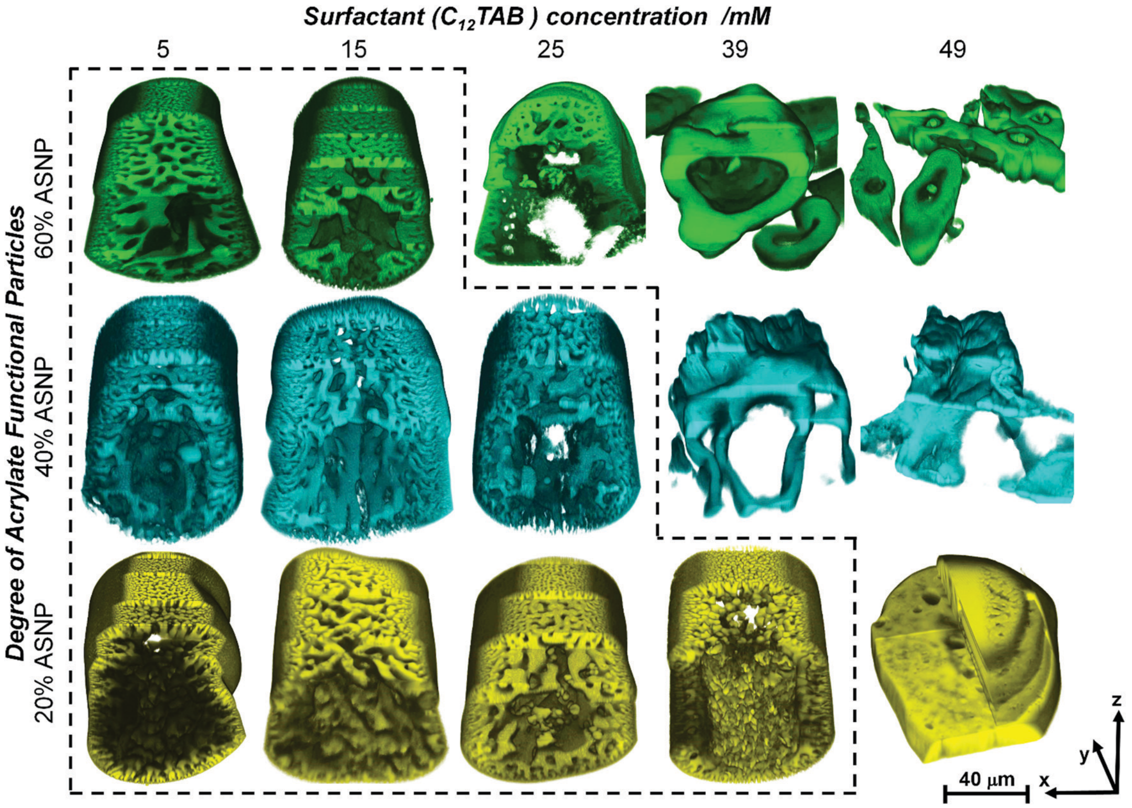

Fig. 4 Asymmetric structures of STrIPS bijel fibers formed with acrylated silica nanoparticles and $C_{12}$TAB. False coloured 3D-reconstructions of STrIPS bijel fiber segments stabilized with nanoparticles of different degrees of acrylation in dependence of the surfactant concentration (dodecyltrimethyldimethyl ammonium bromide ($C_{12}$TAB)). Particles with higher acrylate densities require relatively less surfactant concentrations (as is the case for 60% ASNP, in Fig. 4) to form bijels, whereas particles with lower acrylate densities (*e.g.* 20%-ASNP) can still stabilize bijels when higher surfactant concentrations are added.

### 3.2 Stabilization of bijels with hydrophilic (glycerol functionalized) nanoparticles

Besides hydrophobic particles as stabilizers, potential catalyst particles for the stabilization of bijels can also be of hydrophilic nature. To investigate the requirements to stabilize STrIPS bijels with hydrophilic particles, we employ glycerol functionalized silica particles as model systems. Silica nanoparticles (22 nm diameter) are functionalized with 3-glycidoxypropyltrimethoxy-silane (GPO). The degree of particle functionalization by glycerol groups is controlled to tune the particle wettabilities within the hydrophilic regime. Zeta potential measurements show that the density of the glycerol groups affects the electrophoretic mobility of the functional nanoparticles (Supplementary Note 7, ESI†).

Glycerol-functionalized nanoparticles are not capable of stabilizing bijels on their own, irrespective of the degree of functionalization. Therefore, we test the effect of adding cationic alkylammonium bromide surfactants on the bijel stabilization capability of the particles. The surfactant ($C_{16}$TAB) does not impart enough hydrophobicity to glycerol functionalized nanoparticles for bijel stabilization. We show this by injecting 50 microliters of the ternary mixture with a pipette into water. Fig. 5 shows confocal micrographs of the resulting structures formed with particles of 50% glycerol functionalization.

Increasing the $C_{16}$TAB concentration up to 30 mM in the ternary mixture does not lead to the stabilization of bicontinuous structures. This is likely a consequence of the large amount of hydrophilic hydroxyl (OH) groups on the surface of the nanoparticles. However, we find that viscoelastic nonspherical droplet structures are formed at $\sim$30 mM $C_{16}$TAB, indicating interfacial particle attachment and jamming.

Interestingly, bijels can be stabilized with glycerol functionalized nanoparticles in combination with cationic double chain surfactants. Fig. 5 shows that upon addition of 21 mM didodecyldimethylammonium bromide $(C_{12})_2$TAB to the ternary mixture with glycerol functionalized nanoparticles, bijel-like structures can be obtained.

Furthermore, when the hydrocarbon chain lengths of the dual-chained surfactants are increased (dihexadecyldimethylammonium bromide $(C_{16})_2$TAB), further reduction of the surfactant concentration ($\sim$13 mM) results in the formation of bijel-like structures. Moreover, we observed that for the same type of surfactant ($(C_{16})_2$TAB), higher concentrations were required for higher degrees of glycerol functionalization on the silica nanoparticles (Supplementary Note 8, ESI†). This is likely due to the surfactant adsorption limitations encountered for higher glycerol degrees, as well as the extreme hydrophilicity imparted by the abundance of hydroxyl (OH) groups. As opposed

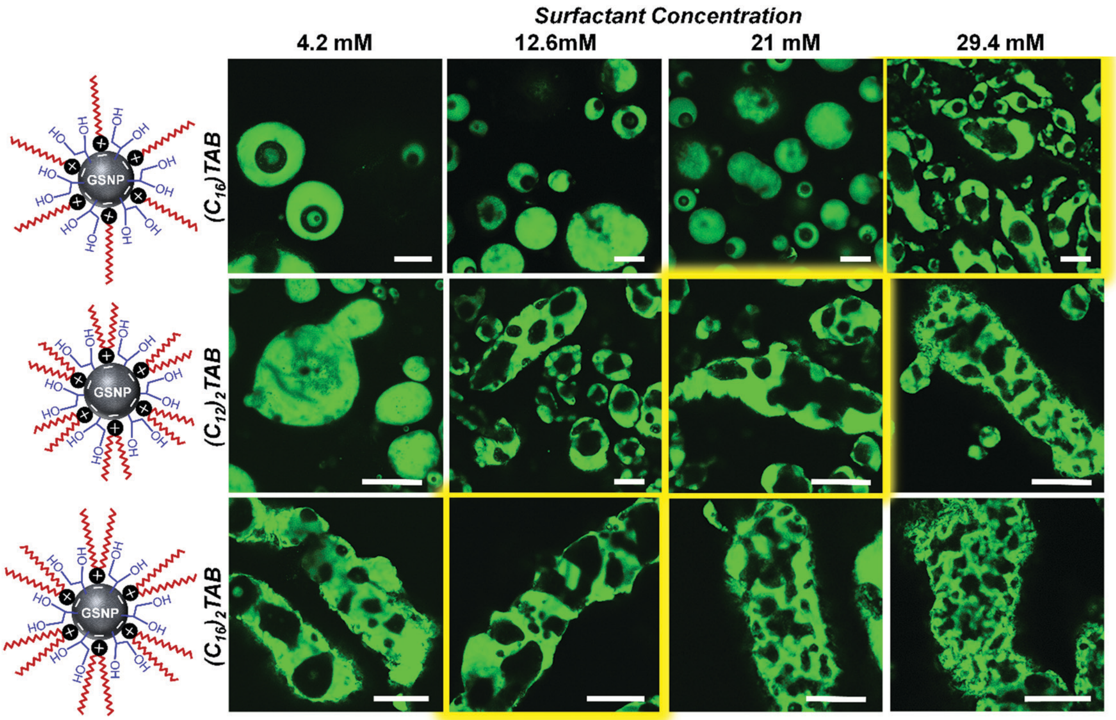

Fig. 5 STrIPS bijels stabilized with hydrophilic glycerol-functionalized silica nanoparticles. Confocal laser scanning microscopy slices of Nile Red dyed emulsion structures formed by glycerol-functionalized silica nanoparticles (50%-GSNPs) and surfactant-functionalized nanoparticles. First row: The single chain surfactants $C_{16}$TAB does not lead to bijel formation, irrespective of the concentration. Second row: Bijel-like structures can be obtained with the double chain surfactants didodecyldimethylammonium bromide ($(C_{12})_2$TAB) above concentrations of 21 mM. Third row: The double chain surfactant dihexadecyldimethylammonium bromide ($(C_{16})_2$TAB) facilitated bijel stabilization at concentrations above 12.6 mM with glycerol-functionalized nanoparticles. Scale bars correspond to 50 μm.

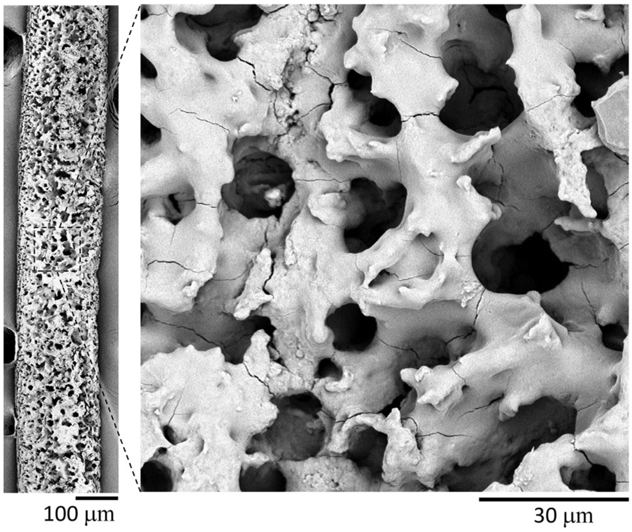

Fig. 6 Scanning Electron Micrograph (SEM) of STrIPS bijel fabricated with glycerol silica nanoparticles (50%-GSNP), showing surface pore openness. 40 mM of the surfactant ($(C_{16})_2$TAB) was used in the ternary mixture composition. The continuous phase contained only 5% v/v of ethanol. On the left, is a piece of the fabricated GSNP-bijel fiber with a corresponding magnified image on the right.

to ASNP bijels with small surface pores ($<2$ μm), bijels made with hydrophilic glycerol particles have significantly open surface pore structures ($\sim$12 μm), as a result of the easy dispersibility of GSNPs in the external continuous water phase (Fig. 6).

## 4 Robust bijels *via* interfacial nanoparticle crosslinking

The confocal micrograph time series in Fig. 7a shows that glycerol particle stabilized bijels coarsen upon adding sodium hydroxide to the continuous water phase (pH increase from 3 to 10). The strongly negatively charged silica surface at pH 10 likely increases the adsorbed amount of $(C_{16})_2$TAB on the particles, changing their contact angle.[29,41] Particles with contact angles deviating from 90 degrees cannot stabilize bicontinuous oil/water channels, as they introduce a preferential curvature to the interface.[2,42]

Stability of bijels against changes in solution pH is achieved by particle cross-linking. We demonstrate this on the example of bijels stabilized with glycerol functionalized nanoparticles. Particle cross-linking is achieved by tolylene 2,4-diisocyanate terminated poly(propylene glycol) (TDPPO, $M_n$ 2300 g mol$^{-1}$) (see schematic in Fig. 7b).[43] TDPPO is added to the initial ternary mixture and the STrIPS process is carried out. TDPPO likely partitions into the BDA rich phase during STRIPS due to its hydrophobic polypropylene spacer. The bijel is stored at room temperature for 12 hours for the reaction of the isocyanate groups with the hydroxyl groups to take place. TDPPO crosslinked

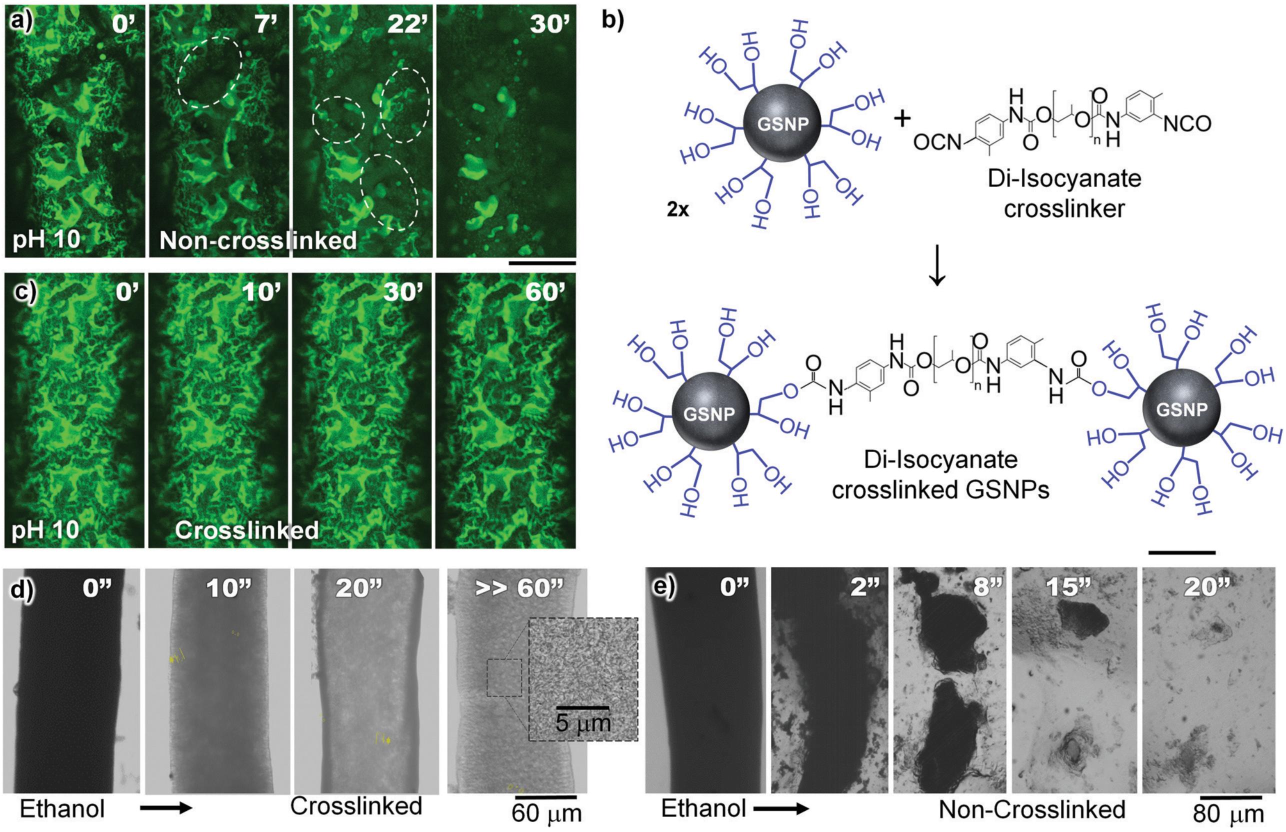

Fig. 7 Robust bijels *via* interfacial nanoparticle crosslinking. (a) Confocal microscopy time series showing coarsening of a glycerol-functionalized particle-stabilized bijel ($(C_{16})_2$TAB modified) upon pH increase. (b) Schematics of isocyanate crosslinking of glycerol-functionalized silica nanoparticles. The isocyanate monomer is dissolved in the oil phase during the ternary mixture preparation prior to bijel fabrication. (c) Confocal microscopy time series showing stability of tolylene 2,4-diisocyanate terminated poly(propylene glycol) (TDPPO) cross-linked bijel upon pH increase. (d) Light microscopy time series showing stability of the nanoparticle scaffold of TDPPO cross-linked bijel upon oil dissolution by ethanol addition. (e) Light microscopy time series of dissolution of glycerol functionalized particle stabilized bijel upon ethanol addition.

bijels are stable under high pH conditions, which is shown by the preservation of the bicontinuous morphology in the time series in Fig. 7c. Furthermore, the robustness of the crosslinked bijels are observed by their stability after remixing the oil and water *via* addition of ethanol to the continuous water phase. After TDPPO cross-linking, ethanol addition dissolves the oil, but the reinforced percolating nanoparticle framework remains intact, as observed *via* light microscopy (Fig. 7d). By increasing the pH of the crosslinked particles following fluid remixing, and subsequently introducing a positively charged dye (rhodamine 110), the preserved bicontinuous scaffold is observed under confocal laser scanning microscopy, which shows that not only is the bijel surface preserved, but the internal regions are as well (see Supplementary Note 9, ESI†). In contrast, the non-crosslinked glycerol particle stabilized bijels collapsed entirely upon the addition of ethanol (Fig. 7e).

## 5 Conclusion

In summary, STrIPS bijel formation was studied with silica nanoparticles of different surface functionalizations to investigate the effect of initial particle wettability on STrIPS bijel stabilization criteria. 3-(Trimethoxysilyl)propyl acrylate-functionalized silica particles were investigated to study bijel stabilization with particles of partially hydrophobic wettability. We find that acrylate-functionalized particles facilitate temporary stabilization of STrIPS bijels on their own. Long-term stability can be imparted by the addition of the mildly hydrophobic cationic surfactant dodecyldimethylammonium bromide. In contrast, our results on STrIPS bijel formation with strongly hydrophilic particles containing 3-glycidoxy-propyltrimethoxysilane groups show the opposite requirement for the surfactant. Here, only highly hydrophobic double chain surfactants (dihexadecyldimethylammonium bromide) facilitate the stabilization of STrIPS bijels. Last, we demonstrate how glycerol-functionalized silica particles facilitate interfacial particle cross-linking by isocyanate chemistry. After cross-linking, structural integrity of the STrIPS bijel nanoparticle scaffold is preserved when pH is increased. This holds true even after remixing of the constituent immiscible fluids of the bijel.

Our study shows how different types of surfactants facilitate the stabilization of bicontinuous emulsions with particles of various initial wettabilities. Our findings will progress future research in designing STrIPS bijel structures by selecting appropriate surfactants for the formation of robust next-generation STrIPS bijels. We are currently investigating methods to obtain fluid transport in robust STrIPS bijels for biphasic applications.

## Author contributions

M. F. H. and S. B.-A. designed the study, S. B.-A. carried out most of the experiments, M. S. S. measured the ternary phase equilibrium. M. F. H. and S. B.-A. wrote the manuscript.

## Conflicts of interest

There are no conflicts to declare.

## Acknowledgements

Acknowledgement is made to the National Science Foundation for support of this research under award number 1751479. This work was supported by NSF-CAREER award number 1751479.

## References

1 K. Stratford, R. Adhikari, I. Pagonabarraga, J. C. Desplat and M. E. Cates, *Science*, 2005, **309**, 2198–2201.
2 E. M. Herzig, K. A. White, A. B. Schofield, W. C. K. Poon and P. S. Clegg, *Nat. Mater.*, 2007, **6**, 966–971.
3 P. S. Clegg, E. M. Herzig, A. B. Schofield, S. U. Egelhaaf, T. S. Horozov, B. P. Binks, M. E. Cates and W. C. K. Poon, *Langmuir*, 2007, **23**, 5984–5994.
4 C. A. L. Colard, R. A. Cave, N. Grossiord, J. A. Covington and S. A. F. Bon, *Adv. Mater.*, 2009, **21**, 2894–2898.
5 M. F. Haase, H. Jeon, N. Hough, J. H. Kim, K. J. Stebe and D. Lee, *Nat. Commun.*, 2017, **8**, 1234.
6 T. J. Thorson, E. L. Botvinick and A. Mohraz, *ACS Biomater. Sci. Eng.*, 2018, **4**, 587–594.
7 S. Zekoll, C. Marriner-Edwards, A. K. O. Hekselman, J. Kasemchainan, C. Kuss, D. E. J. Armstrong, D. Cai, R. J. Wallace, F. H. Richter, J. H. J. Thijssen and P. G. Bruce, *Energy Environ. Sci.*, 2018, **11**, 185–201.
8 J. R. Wilson, J. S. Cronin, A. T. Duong, S. Rukes, H. Y. Chen, K. Thornton, D. R. Mumm and S. Barnett, *J. Power Sources*, 2010, **195**, 1829–1840.
9 M. N. Lee and A. Mohraz, *Adv. Mater.*, 2010, **22**, 4836–4841.
10 J. A. Witt, D. R. Mumm and A. Mohraz, *J. Mater. Chem. A*, 2016, **4**, 1000–1007.
11 D. Cai, F. H. Richter, J. H. J. Thijssen, P. G. Bruce and P. S. Clegg, *Mater. Horiz.*, 2018, **5**, 499–505.
12 J. W. Tavacoli, J. H. J. Thijssen, A. B. Schofield and P. S. Clegg, *Adv. Funct. Mater.*, 2011, **21**, 2020–2027.
13 C. Huang, J. Forth, W. Wang, K. Hong, G. S. Smith, B. A. Helms and T. P. Russell, *Nat. Nanotechnol.*, 2017, **12**, 1060–1063.
14 M. F. Haase, K. J. Stebe and D. Lee, *Adv. Mater.*, 2015, **27**, 7065–7071.
15 D. Cai, P. S. Clegg, T. Li, K. A. Rumble and J. W. Tavacoli, *Soft Matter*, 2017, **13**, 4824–4829.
16 S. Gam, A. Corlu, H. J. Chung, K. Ohno, M. J. A. Hore and R. J. Composto, *Soft Matter*, 2011, **7**, 7262–7268.
17 H. J. Chung, J. Kim, K. Ohno and R. J. Composto, *ACS Macro Lett.*, 2012, **1**, 252–256.
18 L. Bai, J. W. Fruehwirth, X. Cheng and C. W. Macosko, *Soft Matter*, 2015, **11**, 5282–5293.
19 N. Hijnen, D. Cai and P. S. Clegg, *Soft Matter*, 2015, **11**, 4351–4355.
20 L. Imperiali, C. Clasen, J. Fransaer, C. W. Macosko and J. Vermant, *Mater. Horiz.*, 2014, **1**, 139–145.
21 H. Firoozmand and D. Rousseau, *Food Hydrocolloids*, 2015, **48**, 208–212.
22 L. Li, C. Miesch, P. K. Sudeep, A. C. Balazs, T. Emrick, T. P. Russell and R. C. Hayward, *Nano Lett.*, 2011, **11**, 1997–2003.
23 M. F. Haase, N. Sharifi-Mood, D. Lee and K. J. Stebe, *ACS Nano*, 2016, **10**, 6338–6344.
24 P. S. Clegg, *J. Phys.: Condens. Matter*, 2008, **20**, 113101.
25 L. Tran and M. F. Haase, *Langmuir*, 2019, DOI: 10.1021/acs.langmuir.9b00130.
26 Z. G. Cui, L. L. Yang, Y. Z. Cui and B. P. Binks, *Langmuir*, 2010, **26**, 4717–4724.
27 M. Xiao, A. Xu, T. Zhang and L. Hong, *Front. Chem.*, 2018, **6**, 225.
28 M. F. Haase, D. Grigoriev, H. Moehwald, B. Tiersch and D. G. Shchukin, *J. Phys. Chem. C*, 2010, **114**, 17304–17310.
29 A. Maestro, E. Guzmán, E. Santini, F. Ravera, L. Liggieri, F. Ortega and R. G. Rubio, *Soft Matter*, 2012, **8**, 837–843.
30 B. P. Binks and J. A. Rodrigues, *Angew. Chem., Int. Ed.*, 2007, **46**, 5389–5392.
31 Y. Zhu, J. Jiang, K. Liu, Z. Cui and B. P. Binks, *Langmuir*, 2015, **31**, 3301–3307.
32 G. Di Vitantonio, T. Wang, M. F. Haase, K. J. Stebe and D. Lee, *ACS Nano*, 2018, **13**, 26–31.
33 M. Pera-Titus, L. Leclercq, J.-M. Clacens, F. De Campo and V. Nardello-Rataj, *Angew. Chem., Int. Ed.*, 2015, **54**, 2006–2021.
34 W.-J. Zhou, L. Fang, Z. Fan, B. Albela, L. Bonneviot, F. De Campo, M. Pera-Titus and J.-M. Clacens, *J. Am. Chem. Soc.*, 2014, **136**, 4869–4872.
35 L. Leclercq, A. Mouret, A. Proust, V. Schmitt, P. Bauduin, J. M. Aubry and V. Nardello-Rataj, *Chem. – Eur. J.*, 2012, **18**, 14352–14358.
36 Y. Yang, W. J. Zhou, A. Liebens, J. M. Clacens, M. Pera-Titus and P. Wu, *J. Phys. Chem. C*, 2015, **119**, 25377–25384.
37 S. Drexler, J. Faria, M. P. Ruiz, J. H. Harwell and D. E. Resasco, *Energy Fuels*, 2012, **26**, 2231–2241.
38 T. Riittonen, E. Toukoniitty, D. K. Madnani, A.-R. Leino, K. Kordas, M. Szabo, A. Sapi, K. Arve, J. Wärnå and J.-P. Mikkola, *Catalysts*, 2012, **2**, 69–84.
39 E. F. Vansant, P. Van Der Voort and K. C. Vrancken, *Characterization and chemical modification of the silica surface*, Elsevier, 1995, vol. 93.
40 K. V. Peinemann, V. Abetz and P. F. W. Simon, *Nat. Mater.*, 2007, **6**, 992.
41 V. Poulichet and V. Garbin, *Proc. Natl. Acad. Sci. U. S. A.*, 2015, **112**, 5932–5937.
42 M. Destribats, S. Gineste, E. Laurichesse, H. Tanner, F. Leal-Calderon, V. Héroguez and V. Schmitt, *Langmuir*, 2014, **30**, 9313–9326.
43 K. L. Thompson, S. P. Armes, J. R. Howse, S. Ebbens, I. Ahmad, J. H. Zaidi, D. W. York and J. A. Burdis, *Macromolecules*, 2010, **43**, 10466–10474.